Filling the holes in the $CaFe_4As_3$ structure: Synthesis and magnetism of $CaCo_5As_3$

P. F. S. Rosa, B. L. Scott, F. Ronning, E. D. Bauer, and J. D. Thompson
Los Alamos National Laboratory, Los Alamos, New Mexico 87545, USA
(Received 9 May 2017; revised manuscript received 15 June 2017; published 26 July 2017)

Here, we investigate single crystals of $CaCo_5As_3$ by means of single-crystal x-ray diffraction, microprobe, magnetic susceptibility, heat capacity, and pressure-dependent transport measurements. $CaCo_5As_3$ shares the same structure of $CaFe_4As_3$ with an additional Co atom filling a lattice vacancy and undergoes a magnetic transition at $T_M = 16$ K associated with a frustrated magnetic order. $CaCo_5As_3$ displays metallic behavior and its Sommerfeld coefficient ($\gamma = 70$ mJ/mol K^2) indicates a moderate enhancement of electron-electron correlations. Transport data under pressures to 2.5 GPa reveal a suppression of T_M at a rate of -0.008 K/GPa. First-principles electronic structure calculations show a complex three-dimensional band structure and magnetic moments that depend on the local environment at each Co site. Our results are compared with previous data on $CaFe_4As_3$ and provide a scenario for a magnetically frustrated ground state in this family of compounds.

DOI: 10.1103/PhysRevMaterials.1.024409

I. INTRODUCTION

Transition-metal pnictides and chalcogenides have attracted renewed interest in the past decade. From the discovery of high-temperature superconductivity in the Fe-based superconductors [1,2] to the experimental realization of a Weyl semimetal state in TaAs [3–5], these materials have become a promising avenue for the investigation of new states of matter. Although distinct phenomena emerge in different families of transition-metal pnictide compounds, a strong correlation between crystal structure and physical properties is commonplace. In the case of TaAs, spin-orbit coupling and inversion symmetry breaking are key to realizing a Weyl semimetal state. In the case of FeAs-based superconductors, the layered tetragonal structure containing planes of $FeAs_4$ tetrahedra is present in all superconducting families.

The search for new materials not only furthers understanding of the relationship between structure and materials' properties but also can lead to the discovery of new states that emerge from novel structural arrangements. For instance, $CaFe_4As_3$ was synthesized soon after the report of superconductivity in $Ba_{1-x}K_xFe_2As_2$ at $T_c = 38$ K [6,7]. $CaFe_4As_3$ crystallizes in an orthorhombic structure with interpenetrating FeAs strips that also contain $FeAs_4$ tetrahedra. As shown in Fig. 1(a), these strips have a finite width in the ac plane and are connected through fivefold coordinated Fe atoms [Fe(4)], creating channels that host Ca atoms. Thermodynamic measurements on $CaFe_4As_3$ ("143") single crystals reveal a second-order transition at $T_N = 89.6$ K. Neutron diffraction measurements find that the transition at T_N is to a longitudinal ($\|b$) incommensurate (IC) spin-density-wave (SDW) order with a three-dimensional (3D) Heisenberg-like critical exponent [8]. At $T_2 = 25.6$ K, there is a first-order transition to a commensurate order due to the loss of a degree of freedom associated with a soft mode present in the IC state. Band-structure calculations in the nonmagnetic regime appear to be consistent with a nesting instability associated with the planar Fermi sheets from cross-linked FeAs strips [8]. Subsequent first-principles calculations, however, note that the nesting concept would be only valid in the linear perturbation regime over the calculated nonmagnetic state, and, as a consequence, inapplicable for a strongly magnetic state. In fact, the ordered moments extracted from neutron diffraction below T_2 are $2.2\mu_B$ and $2.4\mu_B$ per Fe^{2+} (fourfold) and Fe^{+} (fivefold) sites, respectively. These values are considerably larger than those in Fe-based superconductors (0.4–1μ_B/Fe), but comparable to the moment of strongly correlated FeTe ($2.1\mu_B$) [9]. Moreover, the magnetic structure realized in $CaFe_4As_3$ is similar to that of $Fe_{1.14}Te$ [10].

Theoretical and experimental reports on the FePn-based materials (Pn = pnictogen, chalcogen) show that the Fe moment is sensitive to the Fe-Pn hybridization and tends to increase with increasing Fe-Pn distance [9,11,12]. In fact, the Fe-Te distance in $Fe_{1.14}Te$ (2.59 Å) is comparable to the Fe-As distances in $CaFe_4As_3$ (2.4–2.61 Å) but significantly larger than corresponding distances in the small-moment parent compounds $CaFe_2As_2$ (2.37 Å) and $BaFe_2As_2$ (2.39 Å). Density functional calculations suggest that thicker FePn planes stabilize magnetic structures found in FeTe and $CaFe_4As_3$ due to the effect of bond angles on second- and third-nearest-neighbor interactions [13]. Further, as noted in Ref. [8], the sequence of phase transitions observed in $CaFe_4As_3$ also occurs in $TbMnO_3$ [14] and $Ni_3V_2O_8$ [15], and can be explained by a combination of competing exchange interactions and easy-axis anisotropy. Finally, the simplest of the FeAs-based compounds, FeAs, is highly orthorhombic and also orders in an IC-SDW. First-principles calculations on FeAs show that there is no correspondence whatsoever between the computed real part of the susceptibility and the ordering vector [16]. This result indicates that the common ordering pattern is not nesting driven in these materials. In particular, next-nearest neighbors in FeAs have parallel spins and the Fe-As-Fe bond angle is close to 90° whereas nearest neighbors have opposite spins and much flatter angles, consistent with the Goodenough-Kanamari rules. Though these rules were derived for dielectrics, the observed agreement hints to the presence of local-moment physics.

All of the above suggests a scenario in which magnetic frustration plays a role and IC-SDW order in $CaFe_4As_3$ arises from competing magnetic couplings. Geometrical frustration in metals and insulators has been explored extensively in pyrochlore, kagome, and triangular lattices [17,18], but magnetic frustration also may emerge in the absence of geometrical frustration due solely to competing long-ranged exchange interactions. Experimental examples in tetragonal

systems have been identified recently in Ce-based metals with noncollinear magnetic structures, such as $CeRhIn_5$ and $CeAgBi_2$ [19,20]. A complete understanding of exchange-driven magnetic frustration in transition-metal-based systems without geometrical frustration is, however, still elusive and the question of whether there is a universal way of modeling it in itinerant systems remains unanswered. Magnetic frustration has been proposed to be an important ingredient to describe Fe-based materials [21] and, therefore, the "143" orthorhombic structure and its derivatives may be a good platform to address this question.

Chemical substitution studies together with the investigation of similar parent compounds often provide important insights on the nature of the magnetism in structurally related systems. Previous studies on $Ca(Fe_{1-x}Co_x)_4As_3$ ($0 \leqslant x \leqslant 0.32$) grown in Sn flux showed a slow suppression of the IC-SDW state with x, whereas the IC-C transition rapidly disappeared for $x > 0.1$ [22]. Single crystals with $x > 0.32$ could not be synthesized, which was suggested to be caused by the solubility limit for the 143 structure. We note, however, that the presence of a stable binary compound such as $CoSn_2$ could be detrimental to the formation of the Co 143 analog, and other fluxes may solve this issue.

Here, we report the synthesis of $CaCo_5As_3$ using indium flux. $CaCo_5As_3$ shares the same orthorhombic structure of $CaFe_4As_3$ but has an additional transition-metal site filling the "holes" between Ca atoms. This Co-based compound orders below $T_M = 16$ K in a magnetic state that cannot be ascribed to a simple magnetic structure. $CaCo_5As_3$ is a good metal at low temperatures and applied pressures to 2.5 GPa suppress T_N at a rate of only -0.008 K/GPa. Electron-electron correlations are modest, as evidenced by a Sommerfeld coefficient (γ) of 70 $mJ/mol_{f.u.}\,K^2$. First-principles calculations show a complex three-dimensional band structure in which the magnitude of the magnetic moments depends on the local environment at each Co site. Our results support a scenario in which frustration, driven by competing exchange interactions, play a key role.

Single-crystalline samples of $CaCo_5As_3$ were grown by the In-flux technique. The mixture of elements was placed in an alumina crucible and sealed in a quartz tube under vacuum. The sealed tube was heated to 1000°C for 12 h and then cooled to 400 °C at 6 °C/h. The flux was then removed by centrifugation. The crystallographic structure was verified by single-crystal diffraction at room temperature. In addition, several samples were characterized by elemental analysis using a commercial energy dispersive spectroscopy (EDS) microprobe.

A Quantum Design superconducting quantum interference device and small-mass calorimeter that employs a quasiadiabatic thermal relaxation technique were used to measure magnetic and specific heat properties of the crystals. The electrical resistivity was obtained using a low-frequency ac resistance bridge and a four-contact configuration. Needlelike crystals were mounted in a hybrid piston-cylinder pressure cell with Daphne oil 7373 as the pressure medium. The change in T_c of a piece of Pb served as a manometer. The electronic structure was calculated using density functional theory with an all electron full potential linearized augmented plane wave method with local orbitals. Calculations were implemented in the code WIEN2K using a generalized gradient approximation [23,24]. Spin-orbit coupling was included for computing the density of states.

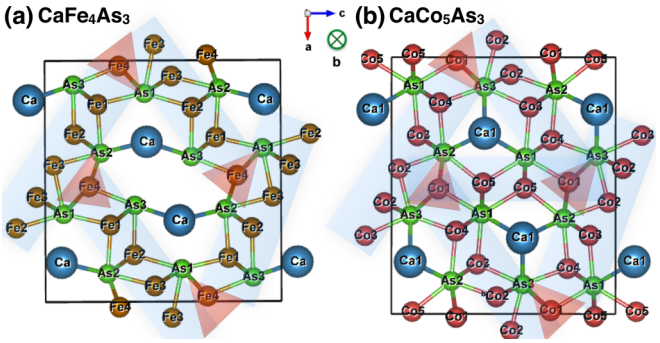

FIG. 1. Crystal structures of (a) $CaFe_4As_3$ [6] and (b) $CaCo_5As_3$ (this work). The elements Ca, Co, Fe, and As are represented by blue, red, gold, and green spheres.

II. RESULTS

Figure 1 shows the orthorhombic crystal structure shared by $CaFe_4As_3$ [6] and $CaCo_5As_3$ (this work). In $CaFe_4As_3$, $FeAs_4$ tetrahedra form infinitely long segments along the b direction. In the ac plane, $FeAs_4$ tetrahedra strips containing structurally inequivalent Fe^{2+} ions [Fe(1), Fe(2), and Fe(3) sites in the blue region] are connected by fivefold Fe^{+1} ions [Fe(4) site] to form a rectangular network that encloses two Ca atoms. Although the same crystal structure is realized in $CaCo_5As_3$, the "hole" between Ca atoms is filled by $CoAs_4$ tetrahedra at the Co(5) site, resulting in a more three-dimensional network with five inequivalent Co sites. We note that $CaFe_5As_3$ can be obtained via high-pressure synthesis and crystallizes in a monoclinic ($P2_1/m$) structure [25]. The physical properties of $CaFe_5As_3$ are unknown, but it is noteworthy that the Fe- and Co-"153" compounds form in different structure types, whereas the Fe-143 and Co-153 materials crystallize in the same space group.

Table I summarizes the structural parameters of $CaCo_5As_3$ determined by single-crystal x-ray diffraction. The lattice parameters are close to those of $CaFe_4As_3$ [$a = 11.852(3)$ Å, $b = 3.7352(6)$ Å, $c = 11.5490(18)$ Å] and the volume of the unit cell increases by 0.5%, likely due to the additional transition-metal site.

Table II displays the atomic coordinates and equivalent displacement parameters for $CaCo_5As_3$. The site symmetries are identical to those found in $CaFe_4As_3$ and the atomic coordinates are also very similar. The refined occupancy of $CaCo_5As_3$ is 100% for all sites, in agreement with the microprobe result $CaCo_{4.9(1)}As_{3.1(1)}$.

Figure 2(a) shows the temperature-dependent magnetic response $M(T)/H$ to a field of 1 kOe applied parallel to the a axis (dark blue squares), b axis (red circles), and c axis (light blue triangles). These results are from zero-field-cooled samples. A clear peak at 16 K for $H \| b$ is characteristic of the onset of antiferromagnetic order. For $H \| a$ and $H \| c$, however, $M(T)/H$ is typical of ferromagnets at the same transition temperature. This clear difference suggests the presence of anisotropic magnetic interactions between Co spins with ferromagnetic and antiferromagnetic components.

TABLE I. Crystallographic data of $CaCo_5As_3$ determined by single-crystal x-ray diffraction.

Crystal system	Orthorhombic
Space group	*Pnma* (62)
Temperature	296(2) K
Wavelength	0.71073 Å
$2\theta_{min}$	2.49°
$2\theta_{max}$	28.43°
Index ranges	$-16 \leqslant h \leqslant 16, -4 \leqslant k \leqslant 5, -14 \leqslant l \leqslant 14$
Formula weight	559.51
a (Å)	12.425(2)
b (Å)	3.8101(6)
c (Å)	10.8513(17)
Volume (Å^3)	513.71(14)
μ (Mo Kα) (cm^{-1})	16.348
Goodness of fit on F^2	1.019
$R(F)$ for $F_o^2 > 2\sigma(F_o^2)$[a]	0.0222
$R_w(F_o^2)$[b]	0.0495

[a] $R(F) = \sum \| F_o| - |F_c\| / \sum |F_o|$.

[b] $R_w(F_o^2) = [\sum [w(F_o^2 - F_c^2)^2] / \sum w F_o^4]^{1/2}$.

Above the ordering temperature where M is linear in H, $M/H \equiv \chi$, the uniform susceptibility. For all directions, $\chi(T)$ can be fit to a Curie-Weiss (CW) law plus a T-independent Pauli term, i.e., $\chi(T) = \chi_0 + C/(T - \theta)$, in the range from 35 to 350 K. The extracted values of χ_0 are 0.004(2) emu/mol$_{f.u.}$ and 0.00257(3) emu/mol$_{f.u.}$ for $H\|a,c$ and $H\|b$, respectively. The effective moment from these fits also is weakly anisotropic, 1.48(3)μ_B/f.u. ($H\|a,c$) and 1.38(1)μ_B/f.u. ($H\|b$), both of which are smaller than the theoretical value expected for Co^{2+} (3.87μ_B using $J = S$). Naively, the effective moment per Co would be 0.26μ_B (from one-fifth of a polycrystalline average of μ_{eff}) but, as we will come to later, the local environment and the hybridization between Co and As atoms are different for each Co site. From the CW fits, the Curie-Weiss temperatures are $\theta = 18(4)$ and 20(2) K for $H\|a,c$ and $H\|b$, respectively. These temperatures are identical within experimental error, positive, which is characteristic of dominant ferromagnetic interactions, and close in value to T_N, typically an indication of little, if any, frustration.

TABLE II. Atomic coordinates and equivalent displacement parameters (Å^2) for $CaCo_5As_3$ determined by single-crystal x-ray diffraction at room temperature. U_{eq} is defined as one third of the trace of the orthogonalized U^{ij} tensor.

Atom	Wyck.	Occ.	x	y	z	U_{eq}
As(1)	4c	1	0.11107	0.25000	0.09824	0.005
As(2)	4c	1	0.12911	0.25000	0.73262	0.005
As(3)	4c	1	0.38532	0.25000	0.91474	0.005
Co(1)	4c	1	0.01244	0.25000	0.29001	0.008
Co(2)	4c	1	0.06633	0.25000	0.53238	0.005
Co(3)	4c	1	0.30513	0.25000	0.11698	0.005
Co(4)	4c	1	0.32191	0.25000	0.71380	0.005
Co(5)	4c	1	0.00960	0.25000	0.90666	0.006
Ca(1)	4c	1	0.29548	0.25000	0.41600	0.006

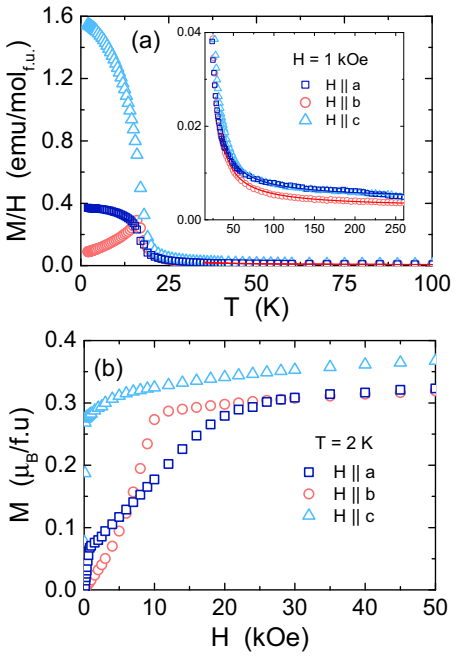

FIG. 2. (a) Temperature dependence of the magnetic response, $M(T)/H$, of $CaCo_5As_3$ in a field of 1 kOe applied along the a, b, and c axes. The inset shows the fits of the high-temperature data to a modified Curie-Weiss law. (b) Anisotropic field dependence of the magnetization at 2 K.

From these parameters that describe the uniform susceptibility, it would be reasonable to expect that $CaCo_5As_3$ could be a simple (Stoner-like) ferromagnet. As evidenced from the sharp peak in $\chi(T)$ for $H\|b$, this simple expectation obviously is incorrect, and the magnetic structure below 16 K must be more complex. A nontrivial magnetic structure is further reflected in the magnetization as a function of magnetic field, shown in Fig. 2(b). For $H\|a$, the magnetization initially increases quickly, as expected for a soft ferromagnetic, but instead of continuing smoothly to saturation, there is a clear anomaly in $M_a(H)$ at ~0.8 kOe, pointing to a change in magnetic structure. At higher fields, $M_a(H)$ smoothly approaches a regime in which it has a small but finite slope $dM/dH = 0.0053$ emu/mol$_{f.u.}$ that is about 1.5 times larger than χ_0 for this orientation. We note that $M_c(H)$ has a similar high-field finite slope. When $H\|b$, $M_b(H)$ increases monotonically at low fields and crosses M_a. At 10 kOe, there is a kink in $M_b(H)$, possibly indicating a change in magnetic structure above which dM/dH approaches a constant value of 0.0063 emu/mol$_{f.u.}$ that is about 2.5 times larger than χ_0. These values of dM/dH above 35 kOe suggest either that the conduction band density of states at the Fermi energy (N_{E_F}) has been Zeeman split (by about 0.2 meV) to give a N_{E_F} that is 1.5–2.5 times larger than at low fields or that there may be one or more additional changes in magnetic structure at fields above 50 kOe. From magnetization and susceptibility measurements, the most likely scenario is that $CaCo_5As_3$ adopts a nontrivial ferrimagnetic order in zero applied field and that its structure is susceptible to field-induced changes.

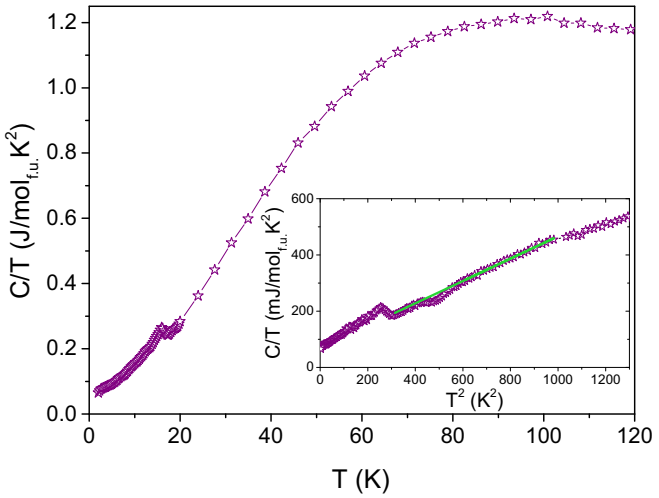

FIG. 3. Specific heat data as a function of temperature. The inset shows a linear fit (solid line) in a C/T vs T^2 plot.

We will return to this possibility, but clearly, high-field measurements as well as microscopic measurements (e.g., neutron diffraction and nuclear magnetic resonance) would be valuable to solve the magnetic structure of $CaCo_5As_3$.

Specific heat data of $CaCo_5As_3$ also display a transition at 16 K (Fig. 3). Above the transition, a fit of the data to $C/T = \gamma + \beta T^2$ yields an electronic coefficient of $\gamma = 70$ mJ/mol$_{f.u.}$ K^2 (inset of Fig. 3). This value of γ should be taken with caution because of the rather small window (15 K) over which the fit was made. Nevertheless, the same fit below T_N also yields $\gamma = 70$ mJ/mol$_{f.u.}$ K^2, in surprising agreement with the high-T value. From these fits above and below T_N, entropy obviously is not conserved, suggesting that there may be another phase transition below the lowest temperature (2 K) of these measurements. Within the free-electron model, the Pauli susceptibility is defined as $\chi_p = \mu_B^2 N(E_F)$, where $N(E_F)$ can be obtained via $\gamma = (1/3)\pi^2 k_B^2 N(E_F)$. Here, μ_B is the Bohr magneton constant and k_B is the Boltzmann constant. Using the high-T experimental value of γ, the calculated Pauli susceptibility is $\chi_p = 1.3 \times 10^{-3}$ emu/f.u., which is smaller than the values of χ_0 obtained from the magnetic susceptibility (2.6×10^{-3} and 3.7×10^{-3} emu/f.u. for $H \| b$ and $H \perp b$, respectively). This simple comparison between χ_p and χ_0 implies that $\chi_0/\gamma > 1$ and suggests that the conduction electrons have ferromagnetic (FM) correlations above T_N.

As shown in Fig. 4(a), the temperature dependence of the electrical resistivity, $\rho(T)$, of $CaCo_5As_3$ along the b axis displays metallic behavior and a curvature that is likely due to scattering of conduction electrons by phonons and s-d interband scattering. The low-T data display a clear kink at T_N, followed by a decrease due to the decrease in spin disorder scattering. The resistance ratio $\rho_{300\,K}/\rho_{2\,K} \sim 25$ is five times larger than that in the Fe-143 counterpart and indicates good crystallinity.

As in $CaFe_4As_3$ [7], there is a Fermi-liquid regime below 15 K where $\rho(T) = \rho_0 + AT^2$ yields a straight line in a ρ vs T^2 plot [bottom inset of Fig. 4(a)]. The extracted values are $\rho_0 = 4.9\ \mu\Omega$ cm and $A = 0.021\ \mu\Omega$ cm K^{-2}. The corresponding Kadowaki-Woods (KW) ratio is $A/\gamma^2 = 9a_0$,

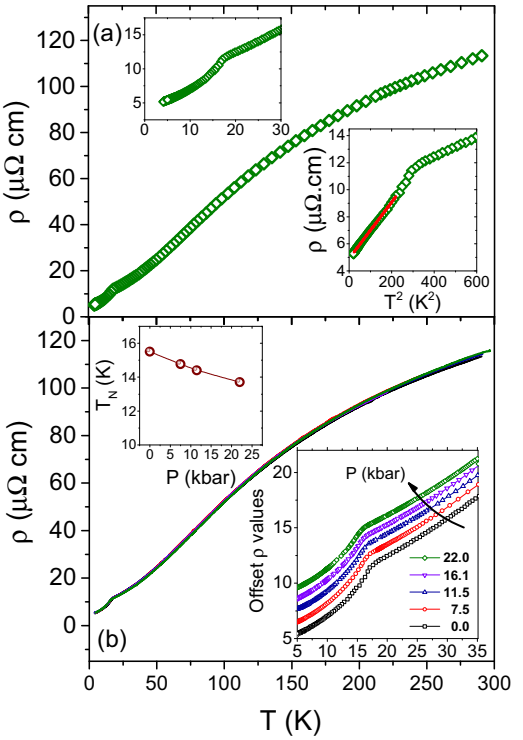

FIG. 4. (a) Electrical resistivity along the b axis, $\rho_b(T)$, of $CaCo_5As_3$ as a function of temperature. The insets plot the low-temperature resistivity vs T and T^2. (b) Pressure dependence of $\rho_b(T)$. The left inset shows the pressure dependence of T_M. The right inset shows the low-T data for various pressures.

where $a_0 = 10^{-5}\ \Omega$ cm mol$_{Co}^2$ K^2 J^{-2} is a universal value observed in strongly correlated materials. This ratio (A/γ^2) is about six times smaller than that for $CaFe_4As_3$, and, not surprisingly, χ_0 is about four times and γ about 1.4 times smaller in $CaCo_5As_3$ compared to $CaFe_4As_3$ [7]. Together, these suggest that electronic correlations are present but not as strong in $CaCo_5As_3$ as they are in isostructural $CaFe_4As_3$.

To investigate whether the magnetic order of $CaCo_5As_3$ can be suppressed to zero temperature, we measured its electrical resistivity as a function of applied pressure. Figure 4(b) shows that the overall temperature dependence of $\rho_b(T)$ does not change significantly with applied pressure. A closer look at the low-temperature region, however, shows that the magnetic transition temperature decreases smoothly as a function of pressure [bottom inset of Fig. 4(b)]. The rate of suppression is rather low (~ -0.008 K/GPa) and higher pressures are necessary to fully suppress the magnetic order.

Electronic structure calculations lend additional support to conclusions drawn from experiments and highlight differences between $CaCo_5As_3$ and $CaFe_4As_3$. Figure 5 displays the density of states of $CaCo_5As_3$ as a function of energy, for which there is a finite density of states at the Fermi level contributed by all five of the Co ions. The associated band dispersion, plotted in Fig. 6(b), is notably three dimensional, and, in particular, planarlike sheets parallel to the b axis present in $CaFe_4As_3$ are absent in our material. From the solely itinerant electron calculations that ignore Coulomb interactions, the calculated $N(E_F) = 14$ states/(f.u. eV) is only about 45% of

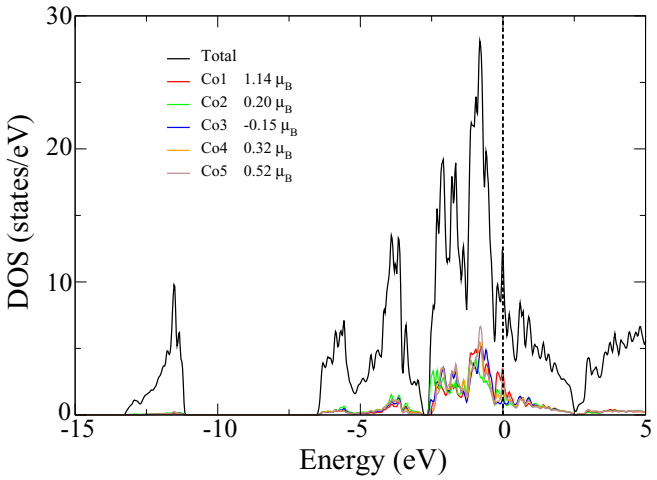

FIG. 5. Total density of states (DOS) as a function of energy as well as the partial contribution from each Co site for a nonmagnetically constrained calculation. The legend provides the moment on each Co site in a spin-polarized calculation.

the density of states obtained from heat capacity [$N(E_F) = 30$ states/(f.u. eV)], and is consistent with a nontrivial role of electronic correlations in $CaCo_5As_3$.

As experimentally measured, the enhanced density of states also suggests a potentially magnetic state. Indeed, spin-polarized calculations find a magnetic ground state. The polarized band-structure calculations give distinct magnetic moments for each Co site [$1.14\mu_B$ on Co(1), $0.20\mu_B$ on Co(2), $-0.15\mu_B$ on Co(3), $0.32\mu_B$ on Co(4), and $0.52\mu_B$ on Co(5)], showing clearly that the moment depends on the local environment of each Co site. Further, these calculations anticipate ferrimagnetic order, as argued from magnetic susceptibility and magnetization measurements to be the likely ordered structure.

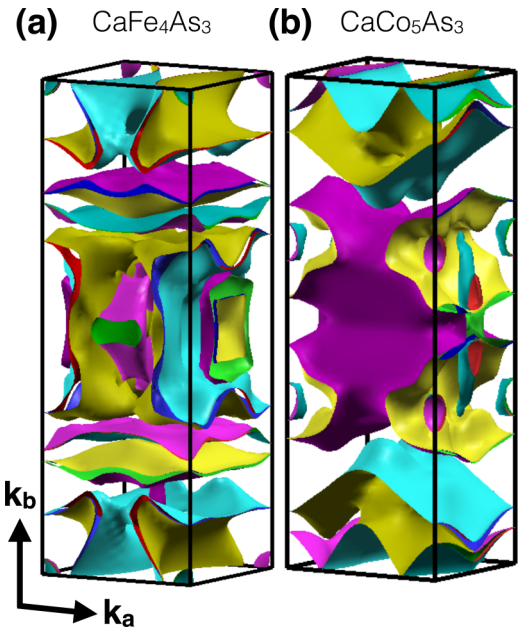

FIG. 6. Fermi surface of (a) $CaFe_4As_3$ and (b) $CaCo_5As_3$.

As mentioned in the Introduction, the Fe moment in the Fe-based superconductors is sensitive to the Fe-As hybridization and tends to increase with increasing Fe-As distance. This tendency is recreated in $CaCo_5As_3$, as the largest magnetic moment is observed at the site with the largest Co-As distance (Co1). The Co-As distances vary from 2.37(6) Å for Co2-5 up to 2.66 Å for Co1. Further, the bond angles Co-As-Co are closer to 90° for nearest neighbors than for next-nearest neighbors, indicating that nearest neighbors have parallel spins and next-nearest neighbors have antiparallel spins. This effect is in agreement with the observed ferromagnetic component and, as in FeAs, is consistent with the Goodenough-Kanamari rules that arise when local-moment physics is present. Thus, our results point to a scenario in which competing exchange interactions in a FM background drive magnetic frustration. This scenario explains the smooth pressure-dependent decrease of T_N because applied pressure is known to increase the hybridization by decreasing the lattice parameters. It will be interesting to investigate whether higher pressures will continuously drive the system to a quantum critical point giving rise to a quantum spin-liquid state. Another possible scenario is that pressure will relieve frustration, resulting in an increase of T_N or a change in the magnetic ground state.

The intricate structure of $CaCo_5As_3$ is further reflected in its Fermi surface, shown in Fig. 6(b). For comparison, we also computed the Fermi surface (FS) of $CaFe_4As_3$ using the structure determined by Ref. [8]. The FS of $CaFe_4As_3$ shown in Fig. 6(a) is in good agreement with that from Ref. [8]. The main difference between the Fermi surfaces of $CaFe_4As_3$ and $CaCo_5As_3$ is the absence of sheets parallel to the b axis in the Co counterpart. Because $CaCo_5As_3$ has one additional Co atom filling the "hole" in the crystal structure, the striplike structure previously seen in $CaFe_4As_3$ is now missing and, as a consequence, no clear sign of "visual" nesting is observed in $CaCo_5As_3$. We speculate that the three dimensionality observed in $CaFe_4As_3$ and $CaCo_5As_3$ is likely responsible for the absence of superconductivity in these materials.

III. CONCLUSIONS

In summary, we have synthesized single crystals of $CaCo_5As_3$, a transition-metal pnictide compound. $CaCo_5As_3$ is a metallic magnet ($T_M = 16$ K) with a moderate enhancement in electronic correlations. Its complex magnetic response indicates competing exchange interactions and magnetic frustration. Electrical resistivity measurements under pressure to 25 kbar show a smooth decrease in T_M to 14 K. Experiments at higher pressures and neutron diffraction measurements will be valuable to fully suppress the magnetic order and to solve the magnetic structure of $CaCo_5As_3$, respectively.

ACKNOWLEDGMENTS

Work at Los Alamos National Laboratory (LANL) was performed under the auspices of the US Department of Energy, Office of Basic Energy Sciences, Division of Materials Science and Engineering. P.F.S.R. acknowledges support via a Director's Postdoctoral Fellowship through the LANL LDRD program.

[1] Y. Kamihara, T. Watanabe, M. Hirano, and H. Hosono, J. Am. Chem. Soc. **130**, 3296 (2008).
[2] M. Rotter, M. Tegel, and D. Johrendt, Phys. Rev. Lett. **101**, 107006 (2008).
[3] S.-Y. Xu *et al.*, Science **349**, 613 (2015).
[4] L. X. Yang *et al.*, Nat. Phys. **11**, 728 (2015).
[5] B. Q. Lv *et al.*, Nat. Phys. **11**, 724 (2015).
[6] I. Todorov *et al.*, J. Am. Chem. Soc. **131**, 5405 (2009).
[7] L. L. Zhao, T. Yi, J. C. Fettinger, S. M. Kauzlarich, and E. Morosan, Phys. Rev. B **80**, 020404(R) (2009).
[8] Y. Nambu, L. L. Zhao, E. Morosan, K. Kim, G. Kotliar, P. Zajdel, M. A. Green, W. Ratcliff, J. A. Rodriguez-Rivera, and C. Broholm, Phys. Rev. Lett. **106**, 037201 (2011).
[9] Z. P. Yin, K. Haule, and G. Kotliar, Nat. Mater. **10**, 932 (2011).
[10] W. Bao, Y. Qiu, Q. Huang, M. A. Green, P. Zajdel, M. R. Fitzsimmons, M. Zhernenkov, S. Chang, M. Fang, B. Qian, E. K. Vehstedt, J. Yang, H. M. Pham, L. Spinu, and Z. Q. Mao, Phys. Rev. Lett. **102**, 247001 (2009).
[11] S. A. J. Kimber *et al.*, Nat. Mater. **8**, 471 (2009).
[12] E. Granado, L. Mendonca-Ferreira, F. Garcia, G. de M. Azevedo, G. Fabbris, E. M. Bittar, C. Adriano, T. M. Garitezi, P. F. S. Rosa, L. F. Bufaical, M. A. Avila, H. Terashita, and P. G. Pagliuso, Phys. Rev. B **83**, 184508 (2011).
[13] C. Y. Moon and H. J. Choi, Phys. Rev. Lett. **104**, 057003 (2010).
[14] M. Kenzelmann, A. B. Harris, S. Jonas, C. Broholm, J. Schefer, S. B. Kim, C. L. Zhang, S. W. Cheong, O. P. Vajk, and J. W. Lynn, Phys. Rev. Lett. **95**, 087206 (2005).
[15] M. Kenzelmann, A. B. Harris, A. Aharony, O. Entin-Wohlman, T. Yildirim, Q. Huang, S. Park, G. Lawes, C. Broholm, N. Rogado, R. J. Cava, K. H. Kim, G. Jorge, and A. P. Ramirez, Phys. Rev. B **74**, 014429 (2006).
[16] S. Zhao, J. M. Mackie, D. E. MacLaughlin, O. O. Bernal, J. J. Ishikawa, Y. Ohta, and S. Nakatsuji, Phys. Rev. B **83**, 180402(R) (2011).
[17] J. S. Gardner, M. J. P. Gingras, and J. E. Greedan, Rev. Mod. Phys. **82**, 53 (2010).
[18] S. Nakatsuji, Y. Nambu, H. Tonomura, O. Sakai, S. Jonas, C. Broholm, H. Tsunetsugu, Y. Qiu, and Y. Maeno, Science **309**, 1697 (2005).
[19] D. Fobes *et al.* (unpublished).
[20] S. M. Thomas, P. F. S. Rosa, S. B. Lee, S. A. Parameswaran, Z. Fisk, and J. Xia, Phys. Rev. B **93**, 075149 (2016).
[21] Q. Si and E. Abrahams, Phys. Rev. Lett. **101**, 076401 (2008).
[22] L. L. Zhao, S. K. Kim, G. T. McCandless, M. S. Torikachvili, P. C. Canfield, J. Y. Chan, and E. Morosan, Phys. Rev. B **84**, 104444 (2011).
[23] P. Blaha, K. Schwarz, G. Madsen, D. Kvasnicka, and J. Luitz, *WIEN2k, An Augmented Plane Wave + Local Orbitals Program for Calculating Crystal Properties* (Technische Universitat Wien, Austria, 2001).
[24] J. P. Perdew, K. Burke, and M. Ernzerhof, Phys. Rev. Lett. **77**, 3865 (1996).
[25] T. Stürzer, C. Hieke, C. Löhnert, F. Nitsche, J. Stahl, C. Maak, R. Pobel, and D. Johrendt, Inorg. Chem. **53**, 6235 (2014).